Received: 4 April 2024 | Revised: 13 June 2024 | Accepted: 16 June 2024

DOI: 10.1002/bit.28786

ARTICLE

BIOTECHNOLOGY AND BIOENGINEERING WILEY

Engineering of Rieske dioxygenase variants with improved *cis*-dihydroxylation activity for benzoates

Phillip C. Betts | **Spencer J. Blakely** | **Bailey N. Rutkowski** | **Brandon Bender** | **Cole Klingler** | **Jordan T. Froese**

Department of Chemistry, Ball State University, Muncie, Indiana, USA

Correspondence
Jordan T. Froese, Department of Chemistry, Ball State University, 1600 W Ashland Ave, Muncie, IN 47303, USA.
Email: jtfroese@bsu.edu

Funding information
Ball State University; National Science Foundation, Grant/Award Number: 2147098

Abstract

Rieske dioxygenases have a long history of being utilized as green chemical tools in the organic synthesis of high-value compounds, due to their capacity to perform the *cis*-dihydroxylation of a wide variety of aromatic substrates. The practical utility of these enzymes has been hampered however by steric and electronic constraints on their substrate scopes, resulting in limited reactivity with certain substrate classes. Herein, we report the engineering of a widely used member of the Rieske dioxygenase class of enzymes, toluene dioxygenase (TDO), to produce improved variants with greatly increased activity for the *cis*-dihydroxylation of benzoates. Through rational mutagenesis and screening, TDO variants with substantially improved activity over the wild-type enzyme were identified. Homology modeling, docking studies, molecular dynamics simulations, and substrate tunnel analysis were applied in an effort to elucidate how the identified mutations resulted in improved activity for this polar substrate class. These analyses revealed modification of the substrate tunnel as the likely cause of the improved activity observed with the best-performing enzyme variants.

KEYWORDS
benzoates, *cis*-dihydroxylation, enzyme engineering, Rieske dioxygenase, substrate tunnel

1 | INTRODUCTION

Rieske dioxygenases (RDOs) are a class of enzymes that play a crucial role in the bacterial metabolism of aromatic compounds in the soil (Abu-Omar et al., 2005; Williams & Sayers, 1994). The metabolic pathways responsible for the degradation of aromatic compounds in these organisms often begin with the RDO-catalyzed regio- and stereoselective dihydroxylation of the aromatic substrate (Figure 1a) (Abu-Omar et al., 2005; Gibson, Koch, Kallio, et al., 1968; Gibson, Koch, Schuld, et al., 1968, 1970; Williams & Sayers, 1994; Ziffer et al., 1977). Owing to the versatility of the *cis*-diol metabolites produced by these enzymes, RDOs rapidly became a popular tool in organic synthesis (Banwell et al., 2003; Boyd & Bugg, 2006; Boyd & Sheldrake, 1998; Hudlicky & Reed, 1995, 2009a, 2009b; Hudlicky & Thorpe, 1996; Lewis, 2014, 2016; Sheldrake, 1992) following the development of transgenic organisms capable of producing these compounds in large quantities (Zylstra & Gibson, 1989). Since this time, over 400 diverse metabolites of RDOs have been characterized (Johnson, 2004), and these metabolites have been applied as building blocks in the synthesis of many valuable compounds (Banwell et al., 2003; Boyd & Bugg, 2006; Boyd & Sheldrake, 1998; Hudlicky & Reed, 1995, 2009a, 2009b; Hudlicky & Thorpe, 1996; Lewis, 2014, 2016; Sheldrake, 1992).

Despite the popularity of RDOs as tools in organic synthesis, their practical utility in this context has been restricted by steric and electronic constraints on their substrate scopes or activity (Froese, Hudlicky, et al., 2014; Newman, et al., 2004; Seo et al., 2013; Osifalujo et al., 2022, 2023; Shainsky et al., 2013; Sheldrake, 1992; Wissner, Schelle, et al., 2021). While some bulky and/or highly polar substrates cannot be metabolized at all by these enzymes

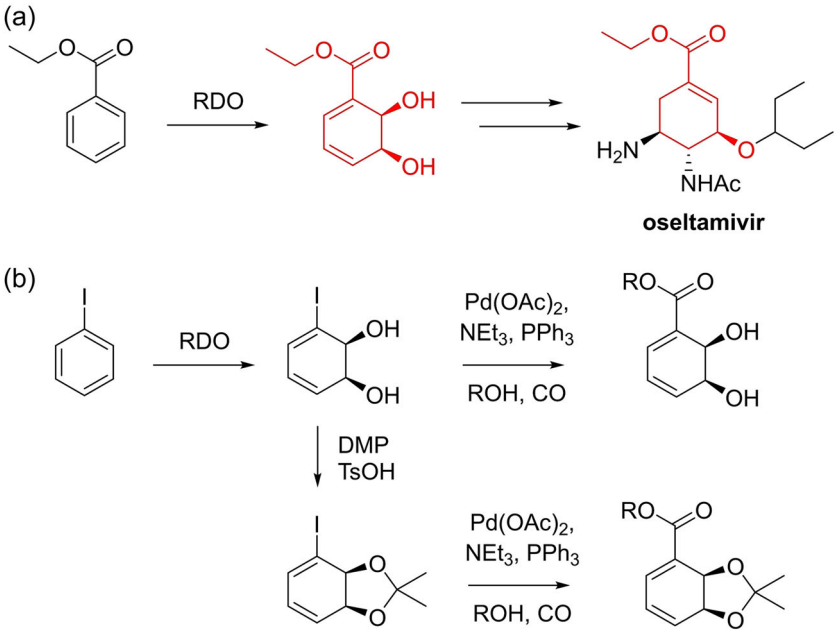

FIGURE 1 (a) Application of the Rieske dioxygenase (RDO)-catalyzed asymmetric dihydroxylation of ethyl benzoate in the synthesis of oseltamivir (Sullivan et al., 2009; Werner et al., 2010). (b) Methodology for the production of ester-functionalized *cis*-diols from RDO metabolites through carbonylation (Froese, Hudlicky, et al., 2014).

(Ang et al., 2009; Froese, Hudlicky, et al., 2014; Keenan et al., 2005; Osifalujo et al., 2023; Seo et al., 2013; Sheldrake, 1992), the sterics and electronics of any potential substrate can also have a considerable impact on the enzyme's activity level (Endoma et al., 2002; Froese, Endoma-Arias, et al., 2014; Johnson, 2004; Osifalujo et al., 2022; Sakamoto et al., 2001; Shainsky et al., 2013; Wissner, Escobedo-Hinojosa, et al., 2021). Although *cis*-diol metabolites produced from aromatics that are metabolized at relatively low rates by RDOs have been utilized in the synthesis of valuable compounds, the poor enzymatic turnover and low-yielding fermentations observed with these substrates hinders the practicality of these syntheses (Baidilov et al., 2018; Endoma-Arias et al., 2014; Makarova et al., 2019; Werner et al., 2010; Winter et al., 2013). To address these limitations in the synthetic utility of RDOs, improved RDO variants have been developed through enzyme engineering that possess expanded substrate scopes or enhanced reactivity in specific contexts (Bernath-Levin et al., 2014; Gally et al., 2015; Newman et al., 2004; Osifalujo et al., 2022, 2023; Seo et al., 2013; Shainsky et al., 2013; Vila et al., 2017; Wissner, Schelle, et al., 2021; Wissner, Escobedo-Hinojosa, et al., 2021; Zhang et al., 2000). Recently, our laboratory has reported rational engineering studies that have produced RDO variants with increased *cis*-dihydroxylation activity for aromatic acetates as well as RDO variants with novel *cis*-dihydroxylation activity for aromatic amides (Osifalujo et al., 2022, 2023). These studies and many others have demonstrated the pliability of the RDO scaffold and the potential for enzyme engineering to expand the practical utility of these enzymes, however many important substrate classes remain unaddressed in this context.

The RDO-derived metabolites of benzoates have demonstrated themselves to be very useful in organic synthesis, having been applied in an efficient synthesis of the antiviral compound oseltamivir (Figure 1a) (Sullivan et al., 2009; Werner et al., 2010), as well as in the production of antiproliferative kibdelone family of compounds (Winter et al., 2013). The fermentation yields for the production of these metabolites using the wild-type enzymes, however, are more than an order of magnitude lower than the yields observed with less polar substrates (Froese, Hudlicky, et al., 2014). This is likely a result of the fact that many of the characterized RDOs have evolved to metabolize nonpolar aromatics such as toluene and naphthalene in their environment (Gibson, Koch, et al., 1968, 1970; Parales & Resnick, 2007; Ziffer et al., 1977), and thus their active sites are organized to bind nonpolar substrates (Friemann et al., 2009; Karlsson et al., 2003). These low fermentation yields have limited the practical utility of syntheses that employ benzoate metabolites as building blocks. In an attempt to overcome these limitations, a methodology has been developed to introduce the ester functional groups into other RDO metabolites through carbonylation (Figure 1b) (Froese, Hudlicky, et al., 2014). The use of this carbonylation methodology, however, increases the number of required synthetic operations, decreasing overall synthetic yields, and relies on toxic heavy metal catalysts. For these reasons, an improved enzymatic catalyst for the *cis*-dihydroxylation of benzoates would be a valuable synthetic tool. Given our previous success in developing RDO variants with improved or expanded reactivity for polar substrates through enzyme engineering (Osifalujo et al., 2022, 2023), our laboratory determined to apply a similar strategy to develop novel RDO variants with improved activity for the *cis*-dihydroxylation of benzoates. The success of such a study would provide new catalytic tools to the synthetic community that would make the application of *cis*-diol metabolites derived from benzoates in organic synthesis much more practical.

2 | MATERIALS AND METHODS

2.1 | General experimental

Escherichia coli BL21 (DE3) competent cells were obtained from ThermoFisher. Plasmid isolation/purification was performed using New England Biolabs Monarch® miniprep kit. Transformations of electro-competent cells were performed on an Eppendorf Eporator®. Whole-cell assay cultures were grown in Greiner Bio-One polystyrene clear, round-bottom 96-well plates. All cultures were incubated in a Barnstead MaxQ 4000 Digital Orbital Incubator Shaker equipped with an Enzyscreen universal clamp system unless otherwise stated. Fluorescence analyses were performed using a Biotek® Synergy™ H1 monochromator-based multi-mode plate reader, using Corning® polystyrene black, opaque, flat-bottom 96-well plates. All reagents were obtained from MilliporeSigma unless otherwise stated. Media were made at pH 7.2 and streptomycin was added at 50 μg mL^{-1}. All *E. coli* cultures were maintained at 37°C unless otherwise stated. NMR analyses were performed using a Jeol ECZ 400S (400 MHz) instrument. Homology modeling was performed using Alphafold2 (Jumper et al., 2021). Docking analyses were performed using AutoDock (Version 4.2.6) (Morris et al., 2009). Molecular dynamics simulations were performed using GROMACS (Abraham et al., 2015; Pronk et al., 2013; van der Spoel et al., 2005). Mapping of active site cavities was performed using PyMOL (Version 2.0 Schrödinger, LLC). Computation and analysis of substrate tunnels were performed using CAVER (version 3.0.3) (Chovancová et al., 2012; Pavelka et al., 2016). Optical rotation analyses were performed by NuMega Labs.

2.2 | Mutant library generation

The pCP-02 expression system was used as the template for toluene dioxygenase (TDO) mutant library generation (Preston-Herrera et al., 2021). Saturation mutagenesis was performed following the procedure of Liu and Naismith (Liu & Naismith, 2008; Zheng, 2004). Amplification was performed using an ABI GeneAmp® 9700 Thermal Cycler. Mutagenic primers were designed according to the procedure of Liu and Naismith (Liu & Naismith, 2008; Zheng, 2004) (see Supporting Information: Table SI for primer sequences). Sequencing analyses were performed by Eurofins Genomics©.

2.3 | Generation of combined mutants

Plasmids bearing beneficial active site mutations generated as part of the study were used as the templates for the introduction of additional mutations. The introduction of point mutations was performed following the procedure of Liu and Naismith (Liu & Naismith, 2008; Zheng, 2004). Amplification was performed using an ABI GeneAmp® 9700 Thermal Cycler. Mutagenic primers were designed according to the procedure of Liu and Naismith (2008) and Zheng (2004) (see Supporting Information: Table SI for primer sequences). Sequencing analyses were performed by Eurofins Genomics©.

2.4 | Whole-cell fermentation 96 well-plate assay protocol

E. coli (BL21 (DE3)) electrocompetent cells were transformed with isolated pCP-02 plasmids expressing TDO (parent and/or mutant libraries), and isolated pCP-01 plasmids as negative controls (Preston-Herrera et al., 2021). The transformation cultures were selected on LB + streptomycin agar plates overnight. Single colonies were inoculated into 160 μL LB + streptomycin media with 0.3% glucose in a 96-well round bottom seed plate and incubated with shaking overnight. All plates included three or more wells containing *E. coli* (BL21 (DE3)) pCP-02 cells expressing the parent TDO enzyme, and three or more wells containing *E. coli* (BL21 (DE3)) pCP-01 (negative control) (Preston-Herrera et al., 2021). Seed plates were used to inoculate 5 μL into 145 μL LB media containing streptomycin in a fresh 96-well round bottom assay plate, and the cultures were incubated with shaking for 2 h 50 min. The assay plates were then pelleted, and the supernatant was discarded. Cultures were resuspended in 140 μL minimal media (KH_2PO_4 – 7.5 g L^{-1}; citric acid – 2 g L^{-1}; $MgSO_4 \cdot 7H_2O$ – 5 g L^{-1}; trace metal solution – 2 mL L^{-1} [Na_2SO_4 – 1 g L^{-1}; $MnSO_4$ – 2 g L^{-1}; $ZnCl_2$ – 2 g L^{-1}; $CoCl_2 \cdot 6H_2O$ – 2 g L^{-1}; $CuSO_4 \cdot 5H_2O$ – 0.3 g L^{-1}; $FeSO_4 \cdot 7H_2O$ – 10 g L^{-1}; pH 1.0]; conc. H_2SO_4 – 1.2 mL L^{-1}; ferric ammonium citrate – 0.3 g L^{-1}; glucose – 4 g L^{-1}; thiamine – 0.034 g L^{-1}; pH 7.2) (Endoma et al., 2002) containing streptomycin and incubated for a 1 h recovery period. Following this, the cultures were induced to a final concentration of 0.5 mM isopropyl β-D-1-thiogalactopyranoside (IPTG), and the incubation temperature was reduced to 30°C. After a 2 h induction period, aromatic substrates were added as 68 mM stock solutions in dimethyl sulfoxide (DMSO) to a final concentration of 2 mM. Cultures were incubated with aromatic substrates for 1.5 h at 30°C, after which the cultures were pelleted. A 100 μL portion of supernatant from each well was transferred to 96-well black opaque assay plates. The reaction was initiated by adding 50 μL of $NaIO_4$ stock solution to each well to a final concentration of 10 mM, and the assay plates were incubated with shaking at room temperature for 30 min. Cleaved diols were detected by adding 50 μL of fluoresceinamine stock solution (prepared with 3 μL conc. HCl (11.65 M)/1 mL fluoresceinamine solution) to each well to a final concentration of 0.1 mM (Preston-Herrera et al., 2021). Assay plates were incubated with shaking at room temperature for 5 h. The fluorescence response from each well was analyzed at 485 nm (ex), 520 nm (em), and normalized to the mean fluorescence response of the negative controls ($[I - I_0]/I_0$).

2.5 | Preparative scale production of methyl (5S,6R)-5,6-dihydroxy-1,3-cyclohexadiene-1-carboxylate

E. coli (BL21 (DE3)) electrocompetent cells were transformed with isolated pCP-02 plasmid containing the TDO genes or relevant mutant version (Preston-Herrera et al., 2021), and selected on LB agar

containing streptomycin overnight. Single colonies were inoculated into 5 mL LB medium containing streptomycin and incubated with shaking overnight. Cultures (2 × 500 mL LB with streptomycin in 2000 mL Erlenmeyer flasks) were inoculated with 5 mL overnight culture each and incubated with shaking. Growth of the cultures was monitored via optical density measurement at 600 nm. Upon reaching an OD600 of 0.5–0.6 AU, 500 mL cultures were pelleted and resuspended in minimal media (KH_2PO_4 – 7.5 g L^{-1}; citric acid – 2 g L^{-1}; $MgSO_4{\cdot}7H_2O$ – 5 g L^{-1}; trace metal solution – 2 mL L^{-1} [Na_2SO_4 – 1 g L^{-1}; $MnSO_4$ – 2 g L^{-1}; $ZnCl_2$ – 2 g L^{-1}; $CoCl_2{\cdot}6H_2O$ – 2 g L^{-1}; $CuSO_4{\cdot}5H_2O$ – 0.3 g L^{-1}; $FeSO_4{\cdot}7H_2O$ – 10 g L^{-1}; pH 1.0]; conc. H_2SO_4 – 1.2 mL L^{-1}; ferric ammonium citrate – 0.3 g L^{-1}; glucose – 4 g L^{-1}; thiamine – 0.034 g L^{-1}; pH 7.2) (Endoma et al., 2002) containing streptomycin. After 1 h of recovery in minimal media, the cultures were induced to a final concentration of 0.5 mM IPTG and the incubation temperature decreased to 30°C. After a 2 h induction period, methyl benzoate was added as a solution in DMSO via pipette to the cultures, in two portions, to a final concentration of 2 mM. The cultures were incubated with the methyl benzoate substrate for 3 h, and subsequently pelleted and the supernatant was decanted. The combined supernatant was then extracted with 3 × 1 L EtOAc, and the combined extracts were dried over anhydrous $MgSO_4$. The dried extract was concentrated and the excess aromatic substrate was removed by filtration through a plug of silica (3:2; EtOAc:hexanes). The resultant solutions were concentrated under reduced pressure to obtain 30–124 mg of methyl (5*S*,6*R*)-5,6-dihydroxy-1,3-cyclohexadiene-1-carboxylate as a clear, colorless oil. Metabolites were dissolved in $CDCl_3$ for ^{1}H NMR analysis (^{1}H NMR (400 MHz, $CDCl_3$) δ 7.06 (d, *J* = 5.5 Hz, 1H), 6.21 (dd, *J* = 9.6, 2.8 Hz, 1H), 6.1 (ddd, *J* = 9.6, 4.8, 2.1 Hz, 1H), 4.58-4.60 (m, 1H), 4.45-4.50 (m, 1H), 3.81 (s, 3H)).

2.6 | Computational visualization of the TDO/TDO variant active sites and substrate tunnels

Homology models were generated using Alphafold2 (Jumper et al., 2021) and AlphaFill (Hekkelman et al., 2023) for analysis of TDO variant active sites and substrate tunnels. The active site cavity in each case was mapped using the surface feature of PyMOL (Version 2.0 Schrödinger, LLC) (cavity detection radius – 3 solvent radii; cavity detection cutoff – 1 solvent radius). Substrate tunnels were computed and analyzed using CAVER (Version 3.0.3) (Chovancova et al., 2012; Pavelka et al., 2016) (minimum probe radius – 0.9; shell depth – 4; shell radius – 3).

2.7 | Enzyme-substrate docking analysis and molecular dynamics simulation

Homology models generated with Alphafold2 (Jumper et al., 2021) and AlphaFill (Hekkelman et al., 2023) were utilized for docking analysis with TDO variants. Enzyme structures were prepared for docking analysis by removing all heteroatoms except the active site iron atom using the "delete atoms" function in AutoDock Tools (Morris et al., 2009). Enzyme structures were further prepared by repairing all missing atoms, adding polar hydrogens, and by adding Kollman charges using the respective functions in AutoDock Tools (Morris et al., 2009). Grid box parameters were set to limit binding to the active site (x = 30 Å, y = 30 Å, z = 30 Å) using AutoDock Tools (Morris et al., 2009). Ligand structures were similarly prepared using AutoDock Tools (Morris et al., 2009). Docking analysis was performed using AutoDock (Version 4.2.6) (Morris et al., 2009). The resultant binding predictions were filtered for binding modes that could result in the successful metabolism of the substrate. All reported binding energies represent the most favorable binding energies among binding modes that could result in the successful metabolism of the substrate. The docking predictions produced were subsequently subjected to molecular dynamics simulations using GROMACS (Abraham et al., 2015; Pronk et al., 2013; van der Spoel et al., 2005). Topologies were generated for both the ligand and enzyme using the CHARMM36 force field (July 2022) (Best et al., 2009; Huang et al., 2016) and the duration of all simulations was 10 ns (5,000,000 steps).

3 | RESULTS AND DISCUSSIONS

3.1 | Engineering of TDO

To identify the optimal template for the engineering of RDO variants with improved activity for benzoates, a series of wild-type RDO enzymes (TDO) from *Pseudomonas putida* F1 (Zylstra & Gibson, 1989), naphthalene dioxygenase (NDO) from *P. putida* G7 (Simon et al., 1993), cumene dioxygenase (CDO) from *P. fluorescens* IP01 (Dong et al., 2005), and biphenyl dioxygenase (BPDO) from *Rhodococcus* strain sp. RHA1 (Furusawa et al., 2004) were screened for their activity on a model substrate (methyl benzoate) using expression platforms for these enzyme systems developed in our laboratory (Preston-Herrera et al., 2021). These screens indicated that among these wild-type enzymes, TDO possessed the greatest baseline activity for this substrate (Supporting Information: Figure S1). Based on this result, TDO was selected as the template for further engineering in this study. With the previous success our laboratory has experienced in improving RDO activity for other substrates by applying a rational mutagenesis approach (Osifalujo et al., 2022, 2023), it was determined that a similar approach would be utilized in this study. To this end, eight active site residues were selected for saturation mutagenesis (M220, A223, L272, I276, V309, L321, I324, and F366; Figure 2). These residues were selected based on their proximity to the substituent of the (native) aromatic substrate when it is bound to the active site (M220 – 4.9 Å, A223 – 3.9 Å, L272 – 5.1 Å, I276 – 5.2 Å, V309 – 4.5 Å, L321 – 3.8 Å, I324 – 4.9 Å, and F366 – 4.3 Å; Figure 2) (Friemann et al., 2009), and based on previous results from our lab and from others (Osifalujo et al., 2022, 2023; Wissner, Schelle, et al., 2021). Using a TDO expression platform developed in our lab as the template

(Preston-Herrera et al., 2021), individual saturation mutagenesis libraries were produced by mutating each of the eight described sites using established methods (Liu & Naismith, 2008; Zheng, 2004). Mutant libraries were then transformed into *E. coli* (BL21 (DE3)) and single colonies were cultured in 96-well plates according to reported protocols (Osifalujo et al., 2022, 2023). Members of each variant library were screened for their *cis*-dihydroxylation activity on two model substrates (methyl benzoate and ethyl benzoate) alongside the parent enzyme and negative controls (pCP-01), using a reported high-throughput, fluorescence-based assay system (Figure 3a) (Preston-Herrera et al., 2021). From these screening studies, five variant libraries

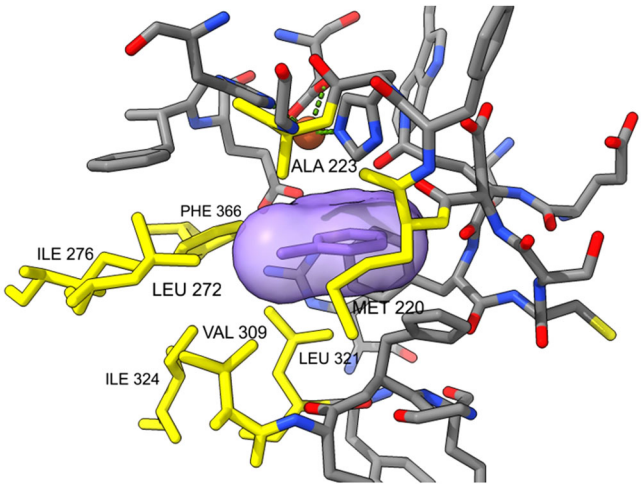

FIGURE 2 Image of the active site of toluene dioxygenase (TDO) with the native substrate (toluene, purple) bound (Friemann et al., 2009). Residues selected for saturation mutagenesis in this study are highlighted (yellow). The mononuclear iron center is shown (orange). Image generated with ChimeraX software (Goddard et al., 2018).

(M220, A223, L272, I276, V309) were shown to contain members that possessed increased activity for either methyl or ethyl benzoate (or both) relative to the parent enzyme. Representative screening data for the L272 variant library is shown in Figure 3b. The validity of all putative "hits" was confirmed through secondary screening before submission for genetic sequencing to identify the nature of any beneficial mutations. These sequencing analyses identified eight point mutations that afforded increased *cis*-dihydroxylation activity for benzoates (M220A, A223V, L272M, L272W, I276C, I276T, I276V, and V309G). Among these mutations, V309G has previously been shown to greatly increase the promiscuity of TDO (Osifalujo et al., 2022, 2023; Wissner, Escobedo-Hinojosa, et al., 2021), and M220A has been shown to improve TDO activity for aromatic acetates and for sterically bulky substrates (Osifalujo et al., 2022; Wissner, Schelle, et al., 2021). I276V has been reported to increase activity for aromatic acetates and confer activity for amide-functionalized aromatics (Osifalujo et al., 2022, 2023), while A223V has been reported to increase activity for sterically bulky substrates (Wissner, Escobedo-Hinojosa, et al., 2021), with L272M and I276T having been shown to increase activity for aromatic acetates (Osifalujo et al., 2022). The L272W mutation is known to confer novel activity for amide-functionalized aromatics (Osifalujo et al., 2023). To our knowledge, the I276C mutation identified in this study has not previously been shown to alter the activity or selectivity of TDO in any previous study.

To accurately determine the relative activity of all the improved TDO variants identified to this point in the study in comparison to the parent enzyme, the *cis*-dihydroxylation activity of all of the described variants for both methyl and ethyl benzoate was tested in parallel, alongside the parent (Figure 4a). These assays determined that the TDO I276V variant possessed the greatest activity for methyl benzoate, while the TDO M220A variant possessed the greatest activity for ethyl benzoate while also demonstrating strong activity

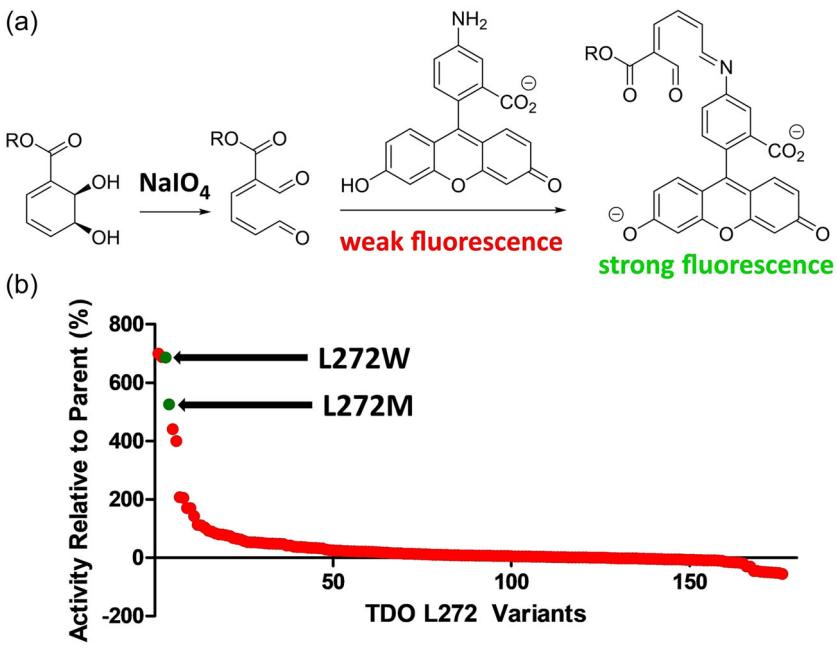

FIGURE 3 (a) Schematic representation of the fluorescence-based assay used to detect and quantify the *cis*-diol metabolites produced by active Rieske dioxygenases (RDOs) (Preston-Herrera et al., 2021); (b) Activity of the toluene dioxygenase (TDO) L272 variant library members for the methyl benzoate substrate relative to the parent enzyme ($n = 176$). Fluorescence response of each variant was normalized to the mean fluorescence response of the negative controls (*E. coli* BL21 (DE3) pCP-01) ($[I - I_0]/I_0$) ($n = 4$) (Preston-Herrera et al., 2021).

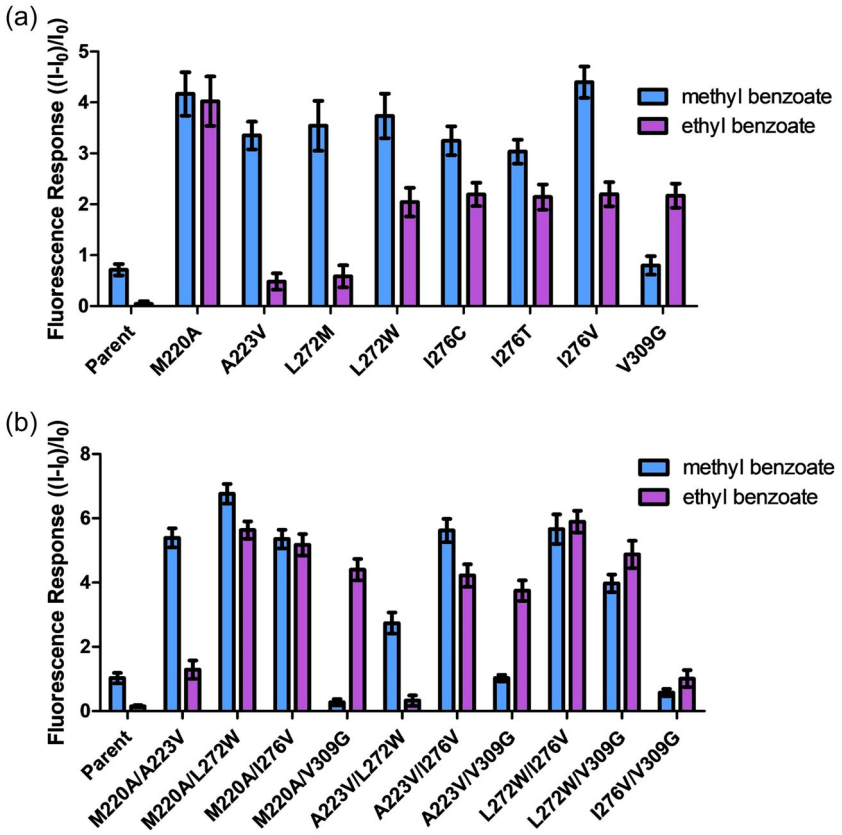

FIGURE 4 (a) Relative activity of variants bearing single active site mutations for ethyl benzoate and methyl benzoate compared to the parent enzyme ($n = 6$). Fluorescence response of each variant was normalized to the mean fluorescence response of the negative controls (*E. coli* BL21 (DE3) pCP-01) ($[I - I_0]/I_0$) ($n = 6$) (Preston-Herrera et al., 2021). (b) Relative activity of doubly combined variants for methyl benzoate and ethyl benzoate compared to the parent enzyme ($n = 6$). Fluorescence response of each variant was normalized to the mean fluorescence response of the negative controls (*E. coli* BL21 (DE3) pCP-01) ($[I - I_0]/I_0$) ($n = 6$) (Preston-Herrera et al., 2021).

for methyl benzoate (Figure 4a). The activity of all these variants for native non-polar substrates (toluene and ethyl benzene) were also tested in parallel, which revealed that every variant retained activity for both substrates, although some of the point mutations (i.e. M220A) resulted in a significant decrease in activity for these substrates (~50% decrease in activity) (Figure S5).

Previous results from our laboratory and others have demonstrated the potential synergistic effects on enzyme activity that can result from combining beneficial point mutations (Osifalujo et al., 2022, 2023; Wissner, Escobedo-Hinojosa, et al., 2021). With this in mind, we determined to iteratively combine the most beneficial mutations identified in the first phase of the study to generate doubly and triply combined mutants. To this end, 10 doubly combined variants (TDO M220A/A223V, TDO M220A/L272W, TDO M220A/I276V, TDO M220A/V309G, TDO A223V/L272W, TDO A223V/I276V, TDO A223V/V309G, TDO L272W/I276V, TDO L272W/V309G, and TDO I276V/V309G) and four triply combined variants (TDO M220A/A223V/L272W, TDO M220A/A223V/I276V, TDO M220A/L272W/I276V, and TDO A223V/L272W/I276V) were produced through established methods (Liu & Naismith, 2008; Zheng, 2004). As was carried out for the single mutants, the activity of all of the doubly combined variants for both methyl and ethyl benzoate was tested in parallel (Figure 4b). These assays did reveal a synergistic effect, with the TDO M220A/L272W variant demonstrating the highest activity for methyl benzoate of any of the variants tested in this study, and the TDO L272W/I276V variant demonstrating the highest activity for ethyl benzoate (Figure 4b). While many of these doubly combined variants showed decreased activity for the native non-polar substrates, the TDO A223V/V309G, TDO L272W/V309G, and TDO I276V/V309G variants were shown to have modest improvements in activity for ethyl benzene relative to the parent (Supporting Information: Figure S6). The synergistic effects observed with the doubly combined variants did not extend to the triply combined variants, however, as all four of these variants demonstrated lower activity for methyl benzoate when compared to any of the variants with single mutations (Supporting Information: Figure S7). The TDO M220A/L272W/I276V variant did possess strong activity for ethyl benzoate, although lower than that of the TDO L272W/I276V variant (Supporting Information: Figure S7). All these triply combined variants also demonstrated reduced activity for the native non-polar substrates relative to the parent enzyme (Supporting Information: Figure S8).

To determine whether the active site mutations introduced into the improved variants identified in this study had any effect on the regio- or enantioselectivity of the enzymatic dihydroxylation, sufficient quantities of the relevant metabolites needed to be produced to facilitate their analysis. To this end, medium-scale (1–2 L) biotransformations were performed with five of the best-performing variants (TDO M220A, TDO I276V, TDO M220A/L272W, TDO L272W/I276V, and TDO A223V/L272W/I276V), as well as the parent enzyme, using methyl benzoate as the substrate. The extracted *cis*-diol metabolites from each of these biotransformations were then compared through ^{1}H NMR and optical rotation analysis. ^{1}H NMR analysis revealed that none of the mutations introduced had any effect on the regioselectivity of the enzymatic transformation

(Supporting Information: Figure S9), and optical rotation analysis revealed minimal effect on the enantioselectivity (Supporting Information: Table SII).

3.2 | Computational analysis of engineered TDO variants

To investigate the cause of the improved activity for methyl and ethyl benzoate observed with the variants produced in this study, homology models of the seven best-performing variants from each phase of this study (TDO M220A, TDO I276V, TDO M220A/L272W, TDO M220A/I276V, TDO A223V/I276V, TDO L272W/I276V, and TDO M220A/L272W/I276V) were constructed using Alphafold2 (Jumper et al., 2021) and the active site iron cofactors added to the predicted structures using AlphaFill (Hekkelman et al., 2023). Previous studies have suggested that certain mutations, including V309G and I276V, can increase the promiscuity of TDO by expanding the binding space in the active site (Osifalujo et al., 2022, 2023; Wissner, Schelle, et al., 2021), facilitating the binding of substrates, such as benzoates, that are sterically larger than the native substrate (toluene). Using the described homology models, the active site cavity was mapped for each variant using PyMOL (Version 2.0 Schrödinger, LLC). This analysis demonstrated that some of the best-performing variants did have expanded binding space in their active sites (TDO M220A/L272W, TDO L272W/I276V), while others had active site cavities similar in size (TDO M220A), or in some cases slightly smaller than (TDO A223V/I276V), the parent enzyme (Figure 5 and Supporting Information: Figure S10). Therefore, the improvement in activity observed among the variants produced in this study could not be solely attributed to expanded active site cavities.

To investigate the binding of the engineered variants, as well as the parent enzyme, to both methyl and ethyl benzoate, docking analyses were performed using Autodock (Version 4.2.6) (Morris et al., 2009). The docking predictions produced from these analyses were then refined through molecular dynamics simulations using GROMACS (Abraham et al., 2015; Pronk et al., 2013; van der Spoel et al., 2005). These analyses did not reveal any correlation between the observed activities of the enzymes and their binding energies (Supporting Information: Table SIII). Modest improvements in binding were observed among some variants for ethyl benzoate following molecular dynamics simulations, including the TDO I276V, A223V/I276V, and L272W/I276V variants, however, these improvements were not observed for the methyl benzoate substrate (Supporting Information: Table SIII). Therefore, these analyses of substrate binding did not provide a satisfactory explanation for the observed improvements in activity over the parent enzyme.

Finally, the structure of the substrate tunnels leading to the active site were investigated for the best-performing variants using CAVER (Chovancova et al., 2012; Pavelka et al., 2016). Computational studies of other RDOs have suggested that the structure of the substrate tunnel leading to the active site, specifically the structure of bottlenecks in the substrate tunnel, can be a primary determinant of the substrate scope of these enzymes (Escalante et al., 2017). Further, modifications of the residues lining the substrate tunnel have been shown to affect the activity/selectivity RDOs (Halder et al., 2018), as well as Rieske (mono)oxygenases (Liu et al., 2022). Mapping of the substrate tunnel in the wild-type enzyme in this way revealed that multiple residues that had been successfully altered to

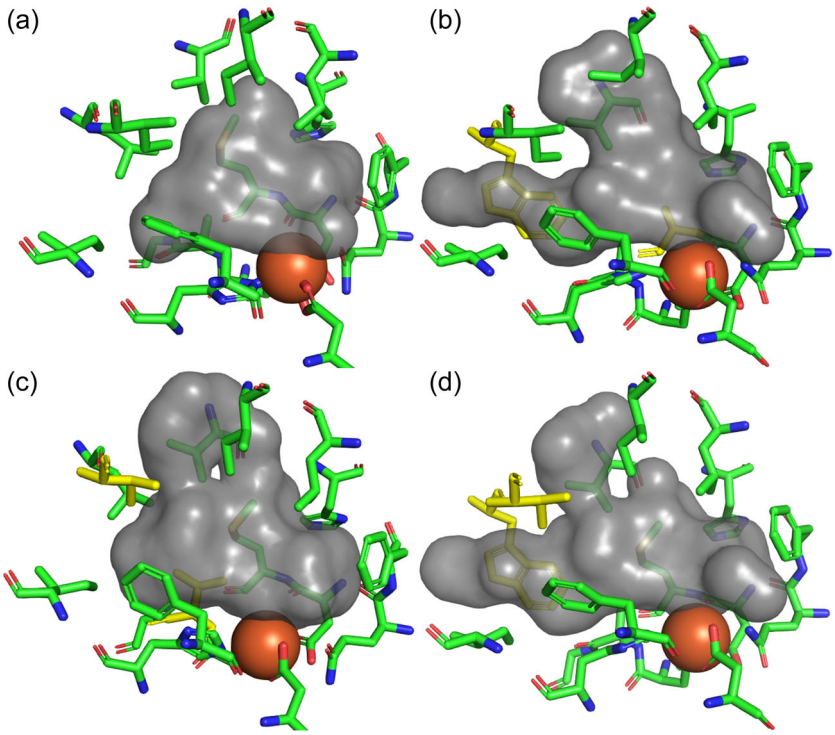

FIGURE 5 Visualization of the active site cavities of toluene dioxygenase (TDO) (wild-type) (a), TDO M220A/L272W (b), TDO A223V/I276V (c), and TDO L272W/I276V (d). Image (a) generated using the reported crystal structure of TDO (Friemann et al., 2009) and with PyMOL (Version 2.0 Schrödinger, LLC). Images (b–d) generated with homology models produced by Alphafold2 (Jumper et al., 2021) and AlphaFill (Hekkelman et al., 2023), and with PyMOL (Version 2.0 Schrödinger, LLC). Mutated residues are highlighted (yellow) and the mononuclear iron center is shown (orange).

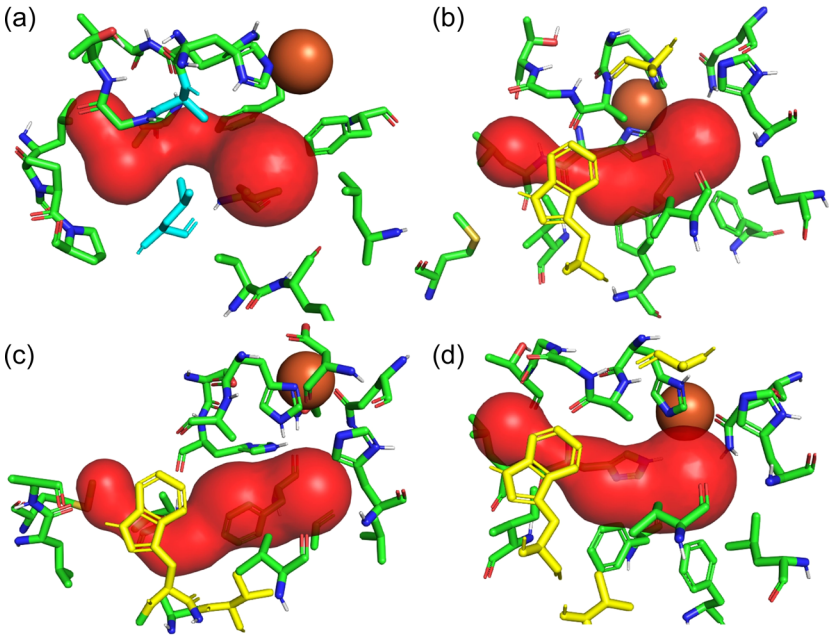

FIGURE 6 Images of the substrate tunnels (red) of TDO (wild-type) (A), TDO M220A/L272W (B), TDO L272W/I276V (C), and TDO M220A/L272W/I276V (D). Overlap of the aromatic indole ring with the substrate tunnel/entrance to the active site cavity is shown for engineered enzymes. Residues at the bottleneck are highlighted (cyan) in the wild-type enzyme. Mutated residues are highlighted for engineered enzymes (yellow) and the mononuclear iron center is shown (orange). Substrate tunnels computed with CAVER (Chovancová et al., 2012; Pavelka et al., 2016) using the reported crystal structure of the wild-type enzyme (Friemann et al., 2009) or with homology models subjected to docking analysis/molecular dynamics simulations (Abraham et al., 2015; Hekkelman et al., 2023; Jumper et al., 2021; Morris et al., 2009; Pronk et al., 2013; van der Spoel et al., 2005). Images generated with PyMOL (Version 2.0 Schrödinger, LLC).

TABLE 1 Characteristics of substrate tunnels as measured by CAVER (Chovancova et al., 2012; Pavelka et al., 2016).

Enzyme	Radius of bottleneck (Å)	Change in bottleneck radius[b]	Cost[a]	Change in cost[b]
TDO (WT)	1.21	-	0.46	-
TDO M220A	1.25	+3%	0.40	−13%
TDO I276V	1.11	−8%	0.52	+13%
TDO M220A/L272W	1.15	−5%	0.40	−13%
TDO M220A/I276V	1.69	+40%	0.27	−41%
TDO A223V/I276V	1.31	+8%	0.37	−20%
TDO L272W/I276V	1.13	−7%	0.45	−2%
TDO M220A/L272W/I276V	1.09	−10%	0.42	−9%

[a]Defined by CAVER to reflect the probability that a pathway is used as a route for the transportation of the substances (Chovancova et al., 2012; Pavelka et al., 2016).

[b]Reported relative to the bottleneck radius/cost calculated for the wild-type enzyme.

improve activity in this study (A223 and L272) existed at the bottleneck of the substrate tunnel (Figure 6a). All the engineered variants analyzed in this way displayed altered substrate tunnels relative to the wild-type enzyme (Supporting Information: Figures S19 and S20). The most illuminating results from these analyses came from the variants bearing the L272W mutation (TDO M220A/L272W, TDO L272W/I276V, and TDO M220A/L272W/I276V), which were some of the best-performing variants identified in this study. These analyses showed that the aromatic indole ring introduced by the leucine-to-tryptophan mutation was positioned adjacent to the substrate tunnel and at the entrance to the active site cavity (Figure 6). Computational studies of the related enzyme naphthalene dioxygenase (NDO) have suggested that a phenylalanine residue positioned at the entrance to the active site cavity in this enzyme plays a role in controlling substrate entrance to the active site by forming stabilizing π–π stacking interactions (Escalante et al., 2017). By analogy, our findings suggest that the improvements in activity observed with engineered variants bearing the L272W mutation may be a result of the introduction of new stabilizing π – π stacking interactions at the entrance to the active site cavity. These analyses also allowed for the radius of the bottlenecks in each substrate tunnel to be measured computationally, and for a "cost" to be associated with each tunnel reflecting the probability of that tunnel being used to transport substrates (Table 1). These measurements showed that the cost associated with the substrate tunnel of every improved variant, except the TDO I276V variant, was reduced relative to the wild-type enzyme (Table 1). In the case of the TDO M220A/I276V variant, the bottleneck in the substrate tunnel was expanded by 40%, which was reflected in the 41% reduction in the cost associated with this substrate

tunnel (Table 1). Taken together, these substrate tunnel analyses provide plausible explanations for the increases in activity observed with many of the engineered variants produced in this study. While these computational analyses have suggested possible explanations for the observed improvements in activity (expanded active site cavities, remodeling of substrate tunnels, and/or the introduction of new stabilizing π–π stacking interactions), a complete picture has not yet been established.

4 | CONCLUSION

In this study, new variants of TDO were rationally engineered that demonstrate considerable improvements in *cis*-dihydroxylation activity for benzoates, the *cis*-diol metabolites of which have demonstrated themselves to be very valuable in organic synthesis (Sullivan et al., 2009; Werner et al., 2010; Winter et al., 2013). To account for the significant improvements in activity observed with these engineered TDO variants, homology modeling, docking analyses, molecular dynamics simulations, and mapping of their substrate tunnels were performed using Alphafold2 (Jumper et al., 2021), AlphaFill (Hekkelman et al., 2023), AutoDock (Morris et al., 2009), GROMACS (Abraham et al., 2015; Pronk et al., 2013; van der Spoel et al., 2005), and CAVER (Chovancova et al., 2012; Pavelka et al., 2016) respectively. Although these studies cannot fully account for the level of activity observed among all the engineered TDO variants, they have provided valuable insights as to the potential source(s) of the observed improvements in activity. These sources may include increases in the size of the TDO binding pocket facilitating the binding of benzoates which are sterically larger than the native substrate, the introduction of new stabilizing π–π stacking interactions at the entrance to the active site/alongside the substrate tunnel, and/or the remodeling of substrate tunnels leading to the active site.

AUTHOR CONTRIBUTIONS

Phillip C. Betts: Enzyme variant screening; construction and screening of combined variants; biotransformation and metabolite isolation/analysis; computational analysis; writing-review and editing. **Spencer J. Blakely**: Mutant library generation; enzyme variant screening; writing-review and editing. **Bailey N. Rutkowski**: Mutant library generation; construction and screening of combined variants; writing-review and editing. **Brandon Bender**: Computational analysis; writing-review and editing. **Cole Klingler**: Biotransformation and metabolite isolation/analysis; writing-review and editing. **Jordan T. Froese**: Conceptualization; funding acquisition; project administration; supervision; writing-original draft; writing-review and editing.

ACKNOWLEDGMENTS

This material is based upon work supported by the National Science Foundation under Grant No. 2147098 (Research in Undergraduate Institutions) and by the Ball State University Junior Faculty Aspire grant program. This work was made possible in part by the Ball State University Provost Start-Up program. The authors would like to thank high-school intern Daniel Yoo for his valuable contributions to this research.

DATA AVAILABILITY STATEMENT

The data that support the findings of this study are available from the corresponding author upon reasonable request.

ORCID

Jordan T. Froese http://orcid.org/0000-0001-6612-4127

REFERENCES

Abraham, M. J., Murtola, T., Schulz, R., Páll, S., Smith, J. C., Hess, B., & Lindahl, E. (2015). GROMACS: High performance molecular simulations through multi-level parallelism from laptops to supercomputers. *SoftwareX*, *1–2*, 19–25. https://doi.org/10.1016/j.softx.2015.06.001

Abu-Omar, M. M., Loaiza, A., & Hontzeas, N. (2005). Reaction mechanisms of mononuclear non-heme iron oxygenases. *Chemical Reviews*, *105*, 2227–2252. https://doi.org/10.1021/cr040653o

Ang, E. L., Obbard, J. P., & Zhao, H. (2009). Directed evolution of aniline dioxygenase for enhanced bioremediation of aromatic amines. *Applied Microbiology and Biotechnology*, *81*, 1063–1070. https://doi.org/10.1007/s00253-008-1710-0

Baidilov, D., Rycek, L., Trant, J. F., Froese, J., Murphy, B., & Hudlicky, T. (2018). Chemoenzymatic synthesis of advanced intermediates for formal total syntheses of tetrodotoxin. *Angewandte Chemie, International Edition*, *57*, 10994–10998. https://doi.org/10.1002/anie.201804602

Banwell, M. G., Edwards, A. J., Harfoot, G. J., Jolliffe, K. A., McLeod, M. D., McRae, K. J., Stewart, S. G., & Vögtle, M. (2003). Chemoenzymatic methods for the enantioselective preparation of sesquiterpenoid natural products from aromatic precursors. *Pure and Applied Chemistry*, *75*, 223–229. https://doi.org/10.1351/pac200375020223

Bernath-Levin, K., Shainsky, J., Sigawi, L., & Fishman, A. (2014). Directed evolution of nitrobenzene dioxygenase for the synthesis of the antioxidant hydroxytyrosol. *Applied Microbiology and Biotechnology*, *98*, 4975–4985. https://doi.org/10.1007/s00253-013-5505-6

Best, R. B., Zhu, X., Shim, J., Lopes, P. E. M., Mittal, J., Feig, M., & MacKerell, Jr., A. D. (2012). Optimization of the additive CHARMM all-atom protein force field targeting improved sampling of the backbone ϕ, ψ and side-chain χ1 and χ2 dihedral angles. *Journal of Chemical Theory and Computation*, *8*, 3257–3273. https://doi.org/10.1021/ct300400x

Boyd, D. R., & Sheldrake, G. N. (1998). The dioxygenase-catalysed formation of vicinal *cis*-diols. *Natural Product Reports*, *15*, 309–324. https://doi.org/10.1039/A815309Y

Boyd, D. R., & Bugg, T. D. (2006). Arene cis-dihydrodiol formation: from biology to application. *Organic & Biomolecular Chemistry*, *4*, 181–192. https://doi.org/10.1039/B513226F

Chovancova, E., Pavelka, A., Benes, P., Strnad, O., Brezovsky, J., Kozlikova, B., Gora, A., Sustr, V., Klvana, M., Medek, P., Biedermannova, L., Sochor, J., & Damborsky, J. (2012). CAVER 3.0: A tool for the analysis of transport pathways in dynamic protein structures. *PLoS Computational Biology*, *8*, e1002708. https://doi.org/10.1371/journal.pcbi.1002708

Dong, X., Fushinobu, S., Fukuda, E., Terada, T., Nakamura, S., Shimizu, K., Nojiri, H., Omori, T., Shoun, H., & Wakagi, T. (2005). Crystal structure of the terminal oxygenase component of cumene dioxygenase from *Pseudomonas fluorescens*. *Journal of Bacteriology*, *187*, 2483–2490. https://doi.org/10.1128/jb.187.7.2483-2490.2005

Endoma, M. A., Bui, V. P., Hansen, J., & Hudlicky, T. (2002). Medium-scale preparation of useful metabolites of aromatic compounds via whole-cell fermentation with recombinant organisms. *Organic Process Research & Development*, *6*, 525–532. https://doi.org/10.1021/op020013s

Endoma-Arias, M. A. A., Hudlicky, J. R., Simionescu, R., & Hudlicky, T. (2014). Chemoenzymatic formal total synthesis of *ent*-codeine and other morphinans via nitrone cycloadditions and/or radical cyclizations. Comparison of strategies for control of C-9/C-14 stereogenic centers. *Advanced Synthesis & Catalysis*, *356*, 333–339. https://doi.org/10.1002/adsc.201400016

Escalante, D. E., Aukema, K. G., Wackett, L. P., & Aksan, A. (2017). Simulation of the bottleneck controlling access into a Rieske active site: predicting substrates of naphthalene 1, 2-dioxygenase. *Journal of Chemical Information and Modeling*, *57*, 550–561. https://doi.org/10.1021/acs.jcim.6b00469

Friemann, R., Lee, K., Brown, E. N., Gibson, D. T., Eklund, H., & Ramaswamy, S. (2009). Structures of the multicomponent Rieske non-heme iron toluene 2,3-dioxygenase enzyme system. *Acta Crystallographica. Section D: Biological Crystallography*, *D65*, 24–33. https://doi.org/10.1107/S0907444908036524

Froese, J., Hudlicky, J. R., & Hudlicky, T. (2014). Palladium-catalyzed carbonylation of halo arene-cis-dihydrodiols to the corresponding carboxylates. Access to compounds unavailable by toluene dioxygenase-mediated dihydroxylation of the corresponding benzoate esters. *Organic & Biomolecular Chemistry*, *12*, 7810–7819. https://doi.org/10.1039/C4OB01417K

Froese, J., Endoma-Arias, M. A. A., & Hudlicky, T. (2014). Processing of *o*-halobenzoates by toluene dioxygenase. The role of the alkoxy functionality in the regioselectivity of the enzymatic dihydroxylation reaction. *Organic Process Research & Development*, *18*, 801–809. https://doi.org/10.1021/op400343c

Furusawa, Y., Nagarajan, V., Tanokura, M., Masai, E., Fukuda, M., & Senda, T. (2004). Crystal structure of the terminal oxygenase component of biphenyl dioxygenase derived from *Rhodococcus* sp. strain RHA1. *Journal of Molecular Biology*, *342*, 1041–1052. https://doi.org/10.1016/j.jmb.2004.07.062

Gally, C., Nestl, B. M., & Hauer, B. (2015). Engineering Rieske non-heme iron oxygenases for the asymmetric dihydroxylation of alkenes. *Angewandte Chemie, International Edition*, *54*, 12952–12956. https://doi.org/10.1002/anie.201506527

Gibson, D. T., Koch, J. R., & Kallio, R. E. (1968). Oxidative degradation of aromatic hydrocarbons by microorganisms. I. Enzymic formation of catechol from benzene. *Biochemistry*, *7*, 2653–2662. https://doi.org/10.1021/bi00847a031

Gibson, D. T., Koch, J. R., Schuld, C. L., & Kallio, R. E. (1968). Oxidative degradation of aromatic hydrocarbons by microorganisms. II. *Biochemistry*, *7*, 3795–3802. https://doi.org/10.1021/bi00851a003

Gibson, D. T., Hensley, M., Yoshioka, H., & Mabry, T. J. (1970). Formation of (+)-*cis*-2,3-dihydroxy-1-methylcyclohexa-4,6-diene from toluene by *Pseudomonas putida*. *Biochemistry*, *9*, 1626–1630. https://doi.org/10.1021/bi00809a023

Goddard, T. D., Huang, C. C., Meng, E. C., Pettersen, E. F., Couch, G. S., Morris, J. H., & Ferrin, T. E. (2018). UCSF ChimeraX: Meeting modern challenges in visualization and analysis. *Protein Science*, *27*, 14–25. https://doi.org/10.1002/pro.3235

Halder, J. M., Nestl, B. M., & Hauer, B. (2018). Semirational engineering of the naphthalene dioxygenase from *Pseudomonas* sp. NCIB 9816-4 towards selective asymmetric dihydroxylation. *ChemCatChem*, *10*, 178–182. https://doi.org/10.1002/cctc.201701262

Hekkelman, M. L., de Vries, I., Joosten, R. P., & Perrakis, A. (2023). AlphaFill: Enriching AlphaFold models with ligands and cofactors. *Nature Methods*, *20*, 205–213. https://doi.org/10.1038/s41592-022-01685-y

Huang, J., Rauscher, S., Nawrocki, G., Ran, T., Feig, M., de Groot, B. L., Grubmüller, H., & MacKerell, Jr., A. D. (2016). CHARMM36m: An improved force field for folded and intrinsically disordered proteins. *Nature Methods*, *14*, 71–73. https://doi.org/10.1038/nmeth.4067

Hudlicky, T., & Reed, J. W. (1995). An evolutionary perspective of microbial oxidations of aromatic compounds in enantioselective synthesis: history, current status, and perspectives. In A. Hassner, *Advances in Asymmetric Synthesis* (pp. 271–312). JAI Press.

Hudlicky, T., & Thorpe, A. J. (1996). Current status and future perspectives of cyclohexadiene-*cis*-diols in organic synthesis: Versatile intermediates in the concise design of natural products. *Chemical Communications*, *17*, 1993–2000. https://doi.org/10.1039/CC9960001993

Hudlicky, T., & Reed, J. W. (2009a). Applications of biotransformations and biocatalysis to complexity generation in organic synthesis. *Chemical Society Reviews*, *38*, 3117–3132. https://doi.org/10.1039/B901172M

Hudlicky, T., & Reed, J. W. (2009b). Celebrating 20 years of SYNLETT - Special account on the merits of biocatalysis and the impact of arene *cis*-dihydrodiols on enantioselective synthesis. *Synlett*. *5*, 685–703. https://doi.org/10.1055/s-0028-1087946

Johnson, R. A. (2004). Microbial arene oxidations. *Organic Reactions*, *63*, 117–264. https://doi.org/10.1002/0471264180.or063.02

Jumper, J., Evans, R., Pritzel, A., Green, T., Figurnov, M., Ronneberger, O., Tunyasuvunakool, K., Bates, R., Žídek, A., Potapenko, A., Bridgland, A., Meyer, C., Kohl, S. A. A., Ballard, A. J., Cowie, A., Romera-Paredes, B., Nikolov, S., Jain, R., Adler, J., … Hassabis, D. (2021). Highly accurate protein structure prediction with AlphaFold. *Nature*, *596*, 583–589. https://doi.org/10.1038/s41586-021-03819-2

Karlsson, A., Parales, J. V., Parales, R. E., Gibson, D. T., Eklund, H., & Ramaswamy, S. (2003). Crystal structure of naphthalene dioxygenase: side-on binding of dioxygen to iron. *Science*, *299*, 1039–1042. https://doi.org/10.1126/science.1078020

Keenan, B. G., Leungsakul, T., Smets, B. F., Mori, M., Henderson, D. E., & Wood, T. K. (2005). Protein engineering of the archetypal nitroarene dioxygenase of *Ralstonia* sp. strain U2 for activity on aminonitrotoluenes and dinitrotoluenes through alpha-subunit residues leucine 225, phenylalanine 350, and glycine 407. *Journal of Bacteriology*, *187*, 3302–3310. https://doi.org/10.1128/jb.187.10.3302-3310.2005

Lewis, S. E. (2014). Applications of biocatalytic arene ipso,ortho *cis*-dihydroxylation in synthesis. *Chemical Communications*, *50*, 2821–2830. https://doi.org/10.1039/C3CC49694E

Lewis, S. E. (2016). Asymmetric dearomatization under enzymatic conditions. In S.-L. You, *Asymmetric dearomatization reactions* (pp. 279–337). Wiley. https://doi.org/10.1002/9783527698479.ch12

Liu, H., & Naismith, J. H. (2008). An efficient one-step site-directed deletion, insertion, single and multiple-site plasmid mutagenesis protocol. *BMC Biotechnology*, *8*, 91. https://doi.org/10.1186/1472-6750-8-91

Liu, J., Tian, J., Perry, C., Lukowski, A. L., Doukov, T. I., Narayan, A. R. H., & Bridwell-Rabb, J. (2022). Design principles for site-selective hydroxylation by a Rieske oxygenase. *Nature Communications*, *13*, 255. https://doi.org/10.1038/s41467-021-27822-3

Makarova, M., Endoma-Arias, M. A. A., Dela Paz, H. E., Simionescu, R., & Hudlicky, T. (2019). Chemoenzymatic total synthesis of *ent-oxycodone: second-, third-, and fourth-generation strategies*. *Journal of the American Chemical Society*, *141*, 10883–10904. https://doi.org/10.1021/jacs.9b05033

Morris, G. M., Huey, R., Lindstrom, W., Sanner, M. F., Belew, R. K., Goodsell, D. S., & Olson, A. J. (2009). AutoDock4 and AutoDockTools4: Automated docking with selective receptor flexibility. *Journal of Computational Chemistry*, *30*, 2785–2791. https://doi.org/10.1002/jcc.21256

Newman, L. M., Garcia, H., Hudlicky, T., & Selifonov, S. A. (2004). Directed evolution of the dioxygenase complex for the synthesis of furanone flavor compounds. *Tetrahedron*, *60*, 729–734. https://doi.org/10.1016/J.tet.2003.10.105

Osifalujo, E. A., Preston-Herrera, C., Betts, P. C., Satterwhite, L. R., & Froese, J. T. (2022). Improving toluene dioxygenase activity for ester-functionalized substrates through enzyme engineering. *ChemistrySelect*, *7*, e202200753. https://doi.org/10.1002/slct.202200753

Osifalujo, E. A., Rutkowski, B. N., Satterwhite, L. R., Betts, P. C., Nkosi, A. K., & Froese, J. T. (2023). Production of novel Rieske dioxygenase metabolites enabled by enzyme engineering. *Catalysis Science & Technology*, *13*, 3784–3790. https://doi.org/10.1039/d3cy00262d

Parales, R. E., & Resnick, S. M. (2007). Biodegradation and bioremediation. In A. Singh, & O. P. Ward (Eds.), *Soil biology* (Vol. 2, pp. 175–195). Springer.

Pavelka, A., Sebestova, E., Kozlikova, B., Brezovsky, J., Sochor, J., & Damborsky, J. (2016). CAVER: Algorithms for analyzing dynamics of tunnels in macromolecules. *IEEE/ACM Transactions on Computational Biology and Bioinformatics*, *13*, 505–517. https://doi.org/10.1109/TCBB.2015.2459680

Preston-Herrera, C., Jackson, A. S., Bachmann, B. O., & Froese, J. T. (2021). Development and application of a high throughput assay system for the detection of Rieske dioxygenase activity. *Organic & Biomolecular Chemistry*, *19*, 775–784. https://doi.org/10.1039/D0OB02412K

Pronk, S., Páll, S., Schulz, R., Larsson, P., Bjelkmar, P., Apostolov, R., Shirts, M. R., Smith, J. C., Kasson, P. M., van der Spoel, D., Hess, B., & Lindahl, E. (2013). GROMACS 4.5: A high-throughput and highly parallel open source molecular simulation toolkit. *Bioinformatics*, *29*, 845–854. https://doi.org/10.1093/bioinformatics/btt055

Sakamoto, T., Joern, J. M., Arisawa, A., & Arnold, F. H. (2001). Laboratory evolution of toluene dioxygenase to accept 4-picoline as a substrate. *Applied and Environmental Microbiology*, *67*, 3882–3887. https://doi.org/10.1128/AEM.67.9.3882-3887.2001

Seo, J., Ryu, J.-Y., Han, J., Ahn, J.-H., Sadowsky, M. J., Hur, H. G., & Chong, Y. (2013). Amino acid substitutions in naphthalene dioxygenase from Pseudomonas sp. strain NCIB 9816-4 result in regio- and stereo-specific hydroxylation of flavanone and isoflavanone. *Applied Microbiology and Biotechnology*, *97*(2), 693–704. https://doi.org/10.1007/s00253-012-3962-y

Shainsky, J., Bernath-Levin, K., Isaschar-Ovdat, S., Glaser, F., & Fishman, A. (2013). Protein engineering of nirobenzene dioxygenase for enantioselective synthesis of chiral sulfoxides. *Protein Engineering, Design and Selection*, *26*, 335–345. https://doi.org/10.1093/protein/gzt005

Sheldrake, G. N. (1992). Biologically derived arene cis-dihydrodiols as synthetic building blocks. In A. N. Collins, G. N. Sheldrake, & J. Crosby (Eds.), *Chirality in industry: The commercial manufacture and application of optically active compounds* (pp. 127–166). John Wiley & Sons Ltd.

Simon, M. J., Osslund, T. D., Saunders, R., Ensley, B. D., Suggs, S., Harcourt, A., Wen-Chen, S., Cruder, D. L., Gibson, D. T., & Zylstra, G. J. (1993). Sequences of genes encoding naphthalene dioxygenase in *Pseudomonas putida* strains G7 and NCIB 9816-4. *Gene*, *127*, 31–37. https://doi.org/10.1016/0378-1119(93)90613-8

van der Spoel, D., Lindahl, E., Hess, B., Groenhof, G., Mark, A. E., & Berendsen, H. J. C. (2005). GROMACS: Fast, flexible, and free. *Journal of Computational Chemistry*, *26*, 1701–1718. https://doi.org/10.1002/jcc.20291

Sullivan, B., Carrera, I., Drouin, M., & Hudlicky, T. (2009). Symmetry-based design for the chemoenzymatic synthesis of oseltamivir (Tamiflu) from ethyl benzoate. *Angewandte Chemie, International Edition*, *48*, 4229–4231. https://doi.org/10.1002/anie.200901345

Vila, M. A., Umpierrez, D., Veiga, N., Seoane, G., Carrera, I., & Giordano, S. R. (2017). Site-directed mutagenesis studies on the toluene dioxygenase enzymatic system: role of phenylalanine 366, threonine 365 and isoleucine 324 in the chemo-, regio-, and stereoselectivity. *Advanced Synthesis & Catalysis*, *359*, 2149–2157. https://doi.org/10.1002/adsc.201700444

Werner, L., Machara, A., & Hudlicky, T. (2010). Short chemoenzymatic azide-free synthesis of oseltamivir (Tamiflu): approaching the potential for process efficiency. *Advanced Synthesis & Catalysis*, *352*, 195–200. https://doi.org/10.1002/adsc.200900844

Williams, P. A., & Sayers, J. R. (1994). The evolution of pathways for aromatic hydrocarbon oxidation in *Pseudomonas*. *Biodegradation*, *5*, 195–217. https://doi.org/10.1007/BF00696460

Winter, D. K., Endoma-Arias, M. A., Hudlicky, T., Beutler, J. A., & Porco, Jr., J. A. (2013). Enantioselective total synthesis and biological evaluation of (+)-kibdelone A and a tetrahydroxanthone analogue. *The Journal of Organic Chemistry*, *78*, 7617–7626. https://doi.org/10.1021/jo401169z

Wissner, J. L., Escobedo-Hinojosa, W., Vogel, A., & Hauer, B. (2021). An engineered toluene dioxygenase for a single step biocatalytical production of (-)-(1S,2R)-*cis*-1,2-dihydro-1,2-naphthalenediol. *Journal of Biotechnology*, *326*, 37–39. https://doi.org/10.1016/j.jbiotec.2020.12.007

Wissner, J. L., Schelle, J. T., Escobedo-Hinojosa, W., Vogel, A., & Hauer, B. (2021). Semi-rational engineering of toluene dioxygenase from *Pseudomonas putida* F1 towards oxyfunctionalization of bicyclic aromatics. *Advanced Synthesis & Catalysis*, *363*, 4905–4914. https://doi.org/10.1002/adsc.202100296

Zhang, N., Stewart, B. G., Moore, J. C., Greasham, R. L., Robinson, D. K., Buckland, B. C., & Lee, C. (2000). Directed evolution of toluene dioxygenase from *Pseudomonas putida* for improved selectivity toward *cis*-indandiol during indene bioconversion. *Metabolic Engineering*, *2*, 339–348. https://doi.org/10.1006/mben.2000.0162

Zheng, L. (2004). An efficient one-step site-directed and site-saturation mutagenesis protocol. *Nucleic Acids Research*, *32*, e115. https://doi.org/10.1093/nar/gnh110

Ziffer, H., Kabuto, K., Gibson, D. T., Kobal, V. M., & Jerina, D. M. (1977). The absolute stereochemistry of several *cis*-dihydrodiols microbially produced from substituted benzenes. *Tetrahedron*, *33*, 2491–2496. https://doi.org/10.1016/0040-4020(77)80070-7

Zylstra, G. J., & Gibson, D. T. (1989). Toluene degradation by *Pseudomonas putida* F1. *The Journal of Biological Chemistry*, *264*, 14940–14946. https://doi.org/10.1016/S0021-9258(18)63793-7

SUPPORTING INFORMATION

Additional supporting information can be found online in the Supporting Information section at the end of this article.

How to cite this article: Betts, P. C., Blakely, S. J., Rutkowski, B. N., Bender, B., Klingler, C., & Froese, J. T. (2024). Engineering of Rieske dioxygenase variants with improved *cis*-dihydroxylation activity for benzoates. *Biotechnology and Bioengineering*, *121*, 3144–3154. https://doi.org/10.1002/bit.28786